Materials Science & Engineering A 730 (2018) 284–294

Contents lists available at ScienceDirect

Materials Science & Engineering A

journal homepage: www.elsevier.com/locate/msea

The effect of tempering temperature on microstructure, mechanical properties and bendability of direct-quenched low-alloy strip steel

Ari Saastamoinen[a,*], Antti Kaijalainen[a], Jouko Heikkala[a], David Porter[a], Pasi Suikkanen[b]

[a] University of Oulu, Centre for Advanced Steels Research, PL 8000, 90014 Oulu, Finland
[b] SSAB Europe Oy, Rautaruukintie 155, 92100 Raahe, Finland

ARTICLE INFO

Keywords:
Martensite
Direct quenching
Tempering
Bendability
Dislocation density
Texture

ABSTRACT

The tempering of re-austenized, quenched and tempered (RAQT) martensitic steels is an extensively studied and well understood field of metallurgy. However, a similar understanding of the effect of tempering on direct-quenched (DQ) high-strength steels has been lacking. Now, for the first time, the effect of tempering in the range of 250–650 °C on the strength, toughness, bendability, microstructure, crystallography and dislocation density of a DQ steel is reported. In the case of tempering at 570 °C, the effects of having a RAQ or DQ starting condition are compared. For the composition and thermal cycles studied, it was found that a peak tempering temperature in the range of 570–600 °C resulted in a DQT steel with an optimal balance of strength, bendability and toughness, i.e. a yield strength greater than 960 MPa, a minimum usable bending radius of 2 times the sheet thickness and T28J of − 50 to − 75 °C depending on the test direction. Crystallographic texture, dislocation density and the distribution of carbides are important factors affecting the bendability of DQT strip. Tempering had no effect on texture, but strongly influenced the size and distribution of carbides thereby resulting in differences in bendability and impact toughness transition temperature.

1. Introduction

The conventional process route for quenched and tempered steels is hot rolling and cooling followed by re-heating, quenching and furnace tempering (RAQT). However, direct quenching (DQ), where the steel plate is directly quenched to martensite after hot rolling, is an interesting energy efficient alternative to the conventional process route as one reheating process is omitted. While conventional RAQT is well understood, the industrially relatively new DQT process requires more research as the state of the austenite prior to quenching can differ substantially from that in conventional quenching and tempering. Furthermore, better understanding for fundamental microstructural differences between RAQT and DQT is valuable in developing new materials.

Already in 1971 Caron and Krauss [1] published an article on the effect of tempering between 400 and 700 °C on the microstructure of 0.2%C RAQT martensite. Krauss continued researching tempered martensite publishing review papers in 1999 [2] and 2017 [3]. In general, RAQT martensite follows a tempering-temperature dependent microstructural evolution including carbon segregation and ε-carbide precipitation (< 200 °C), rod shaped carbide precipitation (200–350 °C) and recovery with spheroidal carbide precipitation (> 330 °C). Regarding mechanical properties, it has been reported that low-temperature tempering leads to an increase in yield strength, tensile strength, hardness and elastic limit until the tempering temperature exceeds 300 °C after which softening processes lead to a decrease in strength. The strength and hardness of martensite increase strongly with increasing carbon content.

The effect of different tempering temperatures on the toughness of RAQT steels has also been studied. Comparisons between low-temperature tempering (LTT) and high-temperature tempering (HTT) were reported by Kennett and Findley [4]. In 1978 Horn and Ritchie [5] described the mechanisms of tempered martensite embrittlement in medium-carbon steels. According to their study, toughness is improved when the tempering temperature is less than 300 °C, whereas toughness is decreased between 300 and 500 °C due to tempered martensite embrittlement, i.e. precipitation of rod-like carbides. On the other hand, in the Gleeble study by Kennett and Findley [4] on the effect of austenite grain size on the properties of quenched and tempered 0.2%C steel, no difference existed in toughness between the quenched and 200 °C tempered (LTT) conditions.

Regardless of the wide and respectable work done by many research

* Corresponding author.
E-mail addresses: ari.saastamoinen@oulu.fi (A. Saastamoinen), antti.kaijalainen@oulu.fi (A. Kaijalainen), jouko.heikkala@oulu.fi (J. Heikkala), david.porter@oulu.fi (D. Porter), pasi.suikkanen@ssab.com (P. Suikkanen).

https://doi.org/10.1016/j.msea.2018.06.014
Received 30 April 2018; Received in revised form 3 June 2018; Accepted 4 June 2018
Available online 05 June 2018

Table 1
Chemical compositions of experimental steel (in wt%).

C	Si	Mn	V	Cr	Mo	Ti	Al	B	P	N	S
0.1	0.2	1.0	0.08	1.0	0.63	0.012	0.03	0.0016	0.006	0.0053	0.0005

groups across world, the effect of tempering temperature on bendability has not yet been reported. Furthermore, the effect of tempering over a wide range of temperatures has not been fully studied in the case of direct quenched steels. An earlier paper [6] showed that high-temperature tempering increased the bendability of DQ steel. Now this paper reports for the first time the effect of different tempering temperatures on the strength, toughness and bendability of DQ steel.

2. Experimental

2.1. Experimental steels

The experimental composition given in Table 1 was cast on a pilot plant. After reheating, slabs were rolled to 6 mm thick strips using a pilot scale hot rolling mill followed by direct quenching. Finishing rolling temperature (FRT) prior to direct quenching was 915 °C, which is above the A_3 austenite-to-ferrite transformation temperature, i.e. 883 °C according to the Andrews' equation [7]. Further details of the rolling procedure are given in the paper by Saastamoinen et al. [8].

To obtain fully re-austenitized and quenched (RAQ) material for comparative studies, DQ specimens were re-austenitized at 910 °C for 30 min and subsequently quenched into a tank of water.

Direct-quenched and tempered (DQT) specimens were produced by tempering the DQ material in a laboratory furnace with peak temperatures at 250, 400, 500, 570, 600 and 650 °C. A slow heating rate of 35 °C/h and no holding time at the peak temperature was employed to simulate the tempering of industrial-scale steel coils. After reaching the peak temperature, specimens were cooled at 40 °C/h to room temperature. To compare the effects caused by the initial microstructure, i.e. DQ or RAQ, RAQT specimens were produced by tempering RAQ material at 570 °C with the same heating and cooling rates. The test matrix is presented in Table 2.

2.2. Microstructural evaluation

To study the evolution of microstructure as a function of tempering temperature, a Zeiss UltraPlus field emission scanning microscope (FESEM) was used. The effect of as-quenched condition, i.e. DQ or RAQ, on texture and grain sizes was revealed with the aid of electron backscatter diffraction (EBSD) measurements and analyses using AZtec*HKL* acquisition and analysis software at both the quarter-thickness position and just below the top surface of the steels. In the EBSD measurements, the FESEM was operated at 15 kV and the step size employed was 0.2 μm. The scanned field size was 80 × 480 μm for subsurface measurements and 80 × 360 μm for quarter thickness measurements.

For EBSD polished samples, X-Ray diffraction (XRD) line broadening studies were carried out at subsurface (150 μm) using Cu K_α radiation on a Rigaku SmartLab 9 kW X-ray diffractometer and PDXL2 analysis software was used to estimate the lattice parameters, microstrains and crystallite sizes of the experimental steels. To determine these parameters, Rietveld refinement was used. As in earlier studies, [6,8], dislocation densities were calculated using the Williamson-Hall method (Eq. (1)) [9,10]:

$$\rho = \sqrt{\rho_s \rho_p} \tag{1}$$

where ρ_s is dislocation density calculated from strain broadening and ρ_p is dislocation density calculated from particle i.e. crystallite size, see Eqs. (2) and (3). According to Williamson et al. [9,10]:

$$\rho_s = \frac{k\varepsilon^2}{Fb^2} \tag{2}$$

and

$$\rho_p = \frac{3n}{D^2} \tag{3}$$

where ε is microstrain, b is burgers vector, F is an interaction factor assumed to be 1, factor k is taken as 14.4 for body-centered cubic metals and D is crystallite size. In Eq. (3), n is the number of dislocations per block face, which is taken as 1. This assumption is based on Williamson et al. [10], as they assume that the metal is broken up into blocks and the dislocations are lying in the boundaries between the blocks. Therefore, n = 1 can be used as an assumption, which will lead to the minimum dislocation density.

Table 2
Experimental matrix.

	Starting condition	Tempering conditions
DQ	Direct-quenched	As-quenched + tempered at 250, 400, 500, 570, 600, 650 °C
RAQ	Re-austenized and quenched	As-quenched + tempered at 570 °C

2.3. Mechanical testing

Three parallel tensile tests were carried out at room temperature for the DQ, DQT and RAQT conditions in accordance with the European standard EN 10002 using flat specimens (6 × 20 × 120 mm^3), cut with their axes both at 0° and 90° to the rolling direction (RD). For specimens both parallel to and transverse to the RD, three Charpy-V experiments at each of six test temperatures from − 140–0 °C were performed with 6 mm thick specimens in the DQ, DQT and RAQT conditions according to the European standard EN 10045.

Tanh-fitting as described by Oldfield [11] using the procedure later introduced by EricksonKirk et al. [12] was used for defining Charpy V transition curves and determining both 28 J transition temperatures and 95% confidence intervals. To convert sub-sized T28J values to full size equivalents, the method presented by Wallin [13,14] was used.

Three-point bending tests were carried out in an Ursviken Optima 100 bending machine to a bending angle of 90 degrees. Plate specimens, 6 × 100 × 300 mm^3, were bent with the bend axes parallel to both the transverse and rolling directions. The die opening width (W) employed was 75 mm and the punch radii (r) ranged from 6 mm to 30 mm. After bending, the quality of the bent surface was examined visually, as described in Ref. [15]. In the evaluation, the formation of a slight nut-shape did not lead to rejection, but if any surface waviness or more severe surface defects appeared, the bend test was considered as failed. The minimum bending radius was that resulting in a defect-free bend.

3. Results and discussion

3.1. Microstructure

3.1.1. The effect of tempering temperature on microstructure of DQ material

Previous studies on the bendability of modern high-strength steels have shown that the microstructure and texture near the surface of the steels are the main factors correlating with bendability [16]. On the

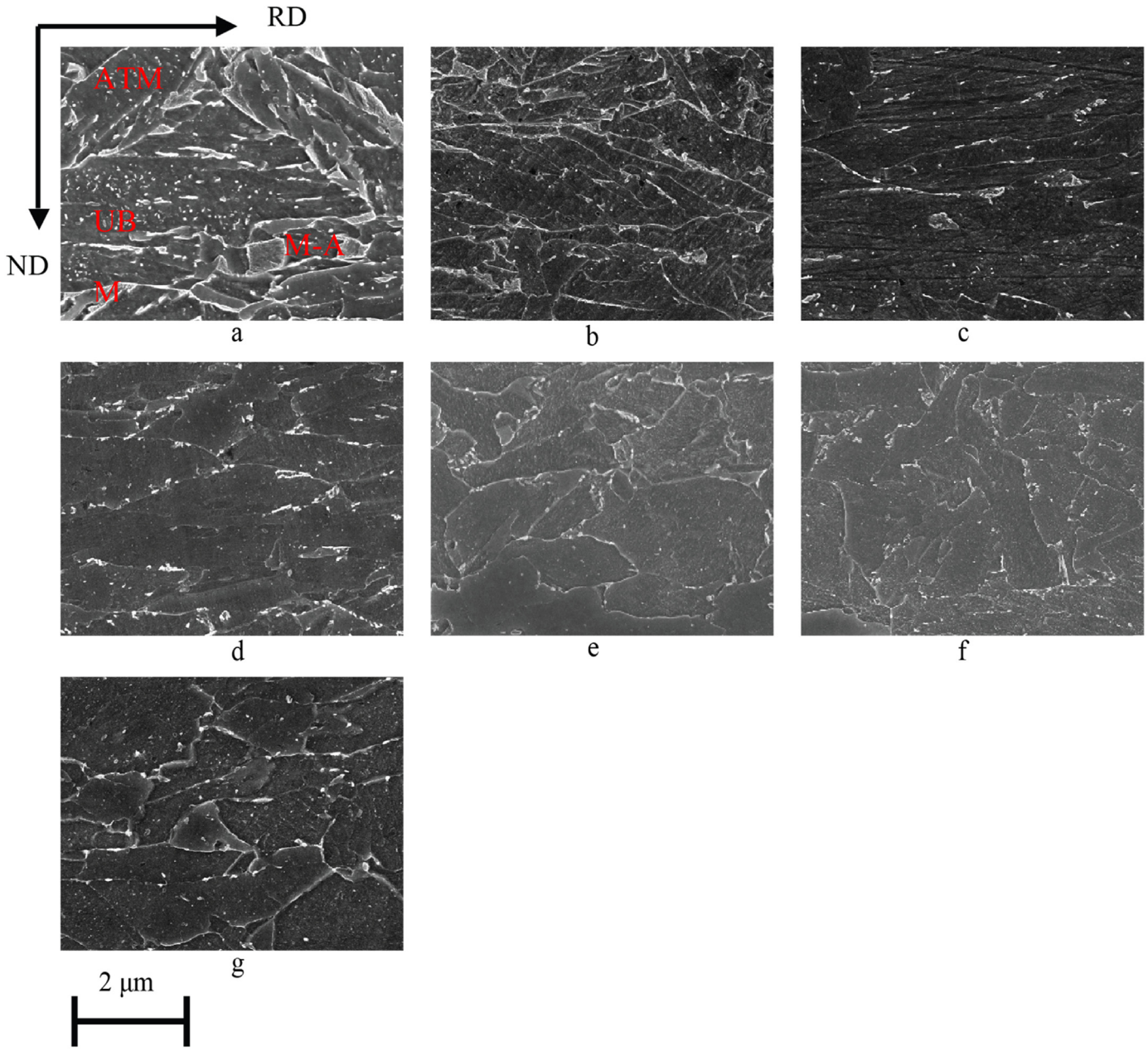

Fig. 1. Subsurface microstructure of (a) DQ, (b) DQT (250 °C), (c) DQT (400 °C), (d) DQT (500 °C), (e) DQT (570 °C), (f) DQT (600 °C) and (g) DQT (650 °C). Nital etched samples with in-lens imaging. Presence of martensite (M), upper bainite (UB), M-A components (M-A) and auto-tempered martensite (ATM) is shown in the direct-quenched condition.

other hand, the microstructure in the bulk determines the overall strength and toughness properties of the steel. Therefore, in this study, subsurface and quarter thickness microstructures are considered separately when discussing the effect of microstructure on strength and impact toughness properties and bendability.

Fig. 1 shows that there is a significant effect of tempering temperature on the microstructure of the DQ condition just below the top surface of the plates. Microstructural characterization showed the presence of martensite, auto-tempered martensite, M-A components and upper bainite in the DQ condition (Fig. 1a). Tempering of this structure in the range 250–500 °C leads to increased carbide precipitation along grain boundaries. However, as could be expected, the carbides started to spheroidize when the tempering temperature was raised to 570–650 °C leading to more uniform and spheroidal carbide structures.

Fig. 2 shows the effect of tempering temperature on the quarter-thickness microstructure of the direct-quenched condition as seen with FESEM in-lens imaging. The microstructure in the direct-quenched condition consists of martensite, auto-tempered martensite and some areas of upper bainite. When tempering is performed at low temperatures, i.e. 250 °C (Fig. 2b), precipitation of fine carbides occurs. These very small carbides are in size region of 2–4 nm and precipitate within the martensite crystals. These are probably transition carbides as presented by Krauss [2] for RAQT steels. As the tempering temperature is increased into the range of 400–500 °C (Fig. 2c-d), the carbides start to grow forming long precipitates in both prior austenite and lath boundaries. This phenomena has earlier been reported to occur for RAQ martensite [5] and the results of this study show that similar microstructural changes occur during the tempering of DQ martensite. When the tempering temperature was increased to 570 °C and above (Fig. 2e-f), carbides, presumably cementite [3,5,17], start to spheroidize and form a uniform carbide structure. As tempering temperature is increased further to 650 °C (Fig. 2g), the cementite coarsens and

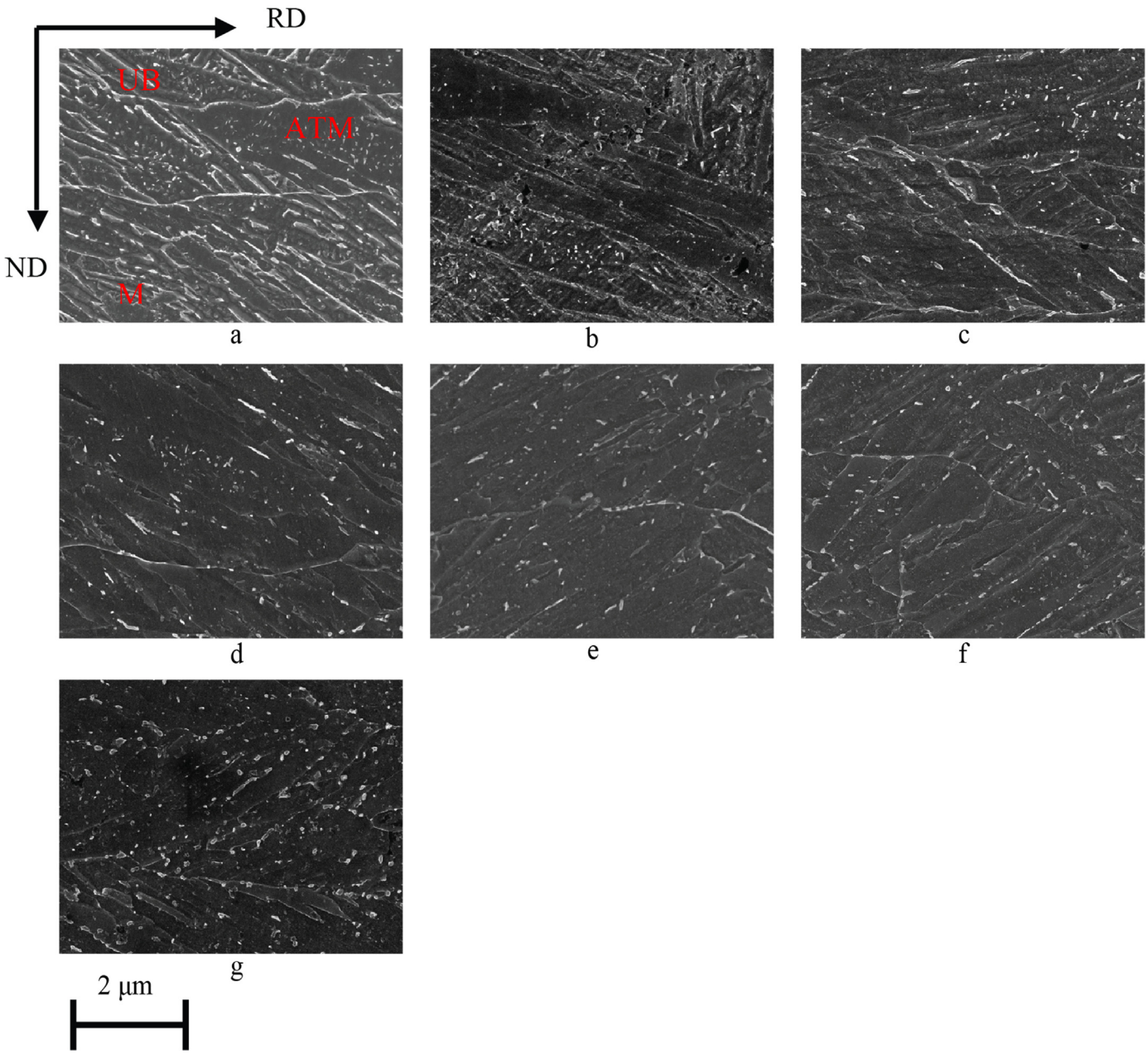

Fig. 2. Quarter-thickness microstructures of (a) DQ, (b) DQT (250 °C), (c) DQT (400 °C), (d) DQT (500 °C), (e) DQT (570 °C), (f) DQT (600 °C) and (g) DQT (650 °C). Nital etched samples with in-lens imaging. Presence of martensite (M), upper bainite (UB) and auto-tempered martensite (ATM) is shown in the direct-quenched condition.

spheroidizes even further.

3.1.2. EBSD studies

Subsurface EBSD inverse pole figure (IPF) maps for the RD direction in the DQ samples are presented in Fig. 3. From the IPF maps, it can be seen that the subsurface grains of the DQ steel are elongated in the rolling direction. For the RAQ steel, the grain structure is equiaxed as is typical for re-austenitized materials.

Fig. 4 shows the main texture components of the BCC structure in the $\varphi_2 = 45^\circ$ ODF section, while Fig. 5 shows the texture intensities in corresponding sections for the RAQ and DQ conditions. The intense shear texture component $\{112\} < 111 >_\alpha$ for the DQ state is absent in the RAQ state. Strong shear texture components are expected to form in the austenite close to the rolled surfaces, i.e., $\{111\} < 211 >_\gamma$ and $\{112\} < 110 >_\gamma$. After cooling and phase transformation these lead to the formation of the BCC shear components $\{112\} < 111 >_\alpha$, and $\{110\} < 111 >_\alpha$, respectively [18]. As the prior austenite grain structure of the DQ condition is elongated, it appears that the final hot rolling passes have been made below the recrystallization stop temperature. The ODF sections in Fig. 5 show that tempering reduces the maximum intensities of the main texture components, especially in the case of the DQ state. It was not possible, however, to relate these changes to changes in the grain structure of the steel that might have been caused by e.g. recrystallization during the long tempering treatment. The observed texture intensity change is, however, consistent with an earlier study showing that tempering reduces peak texture intensities in the case of DQ high-strength steels. [6] More systematic studies on the effect of high temperature tempering parameters on the texture of DQ martensite are needed, as no such studies have been published.

The subsurface grain boundary misorientation distributions in Fig. 6a show some difference between RAQ and DQ steels. The DQ

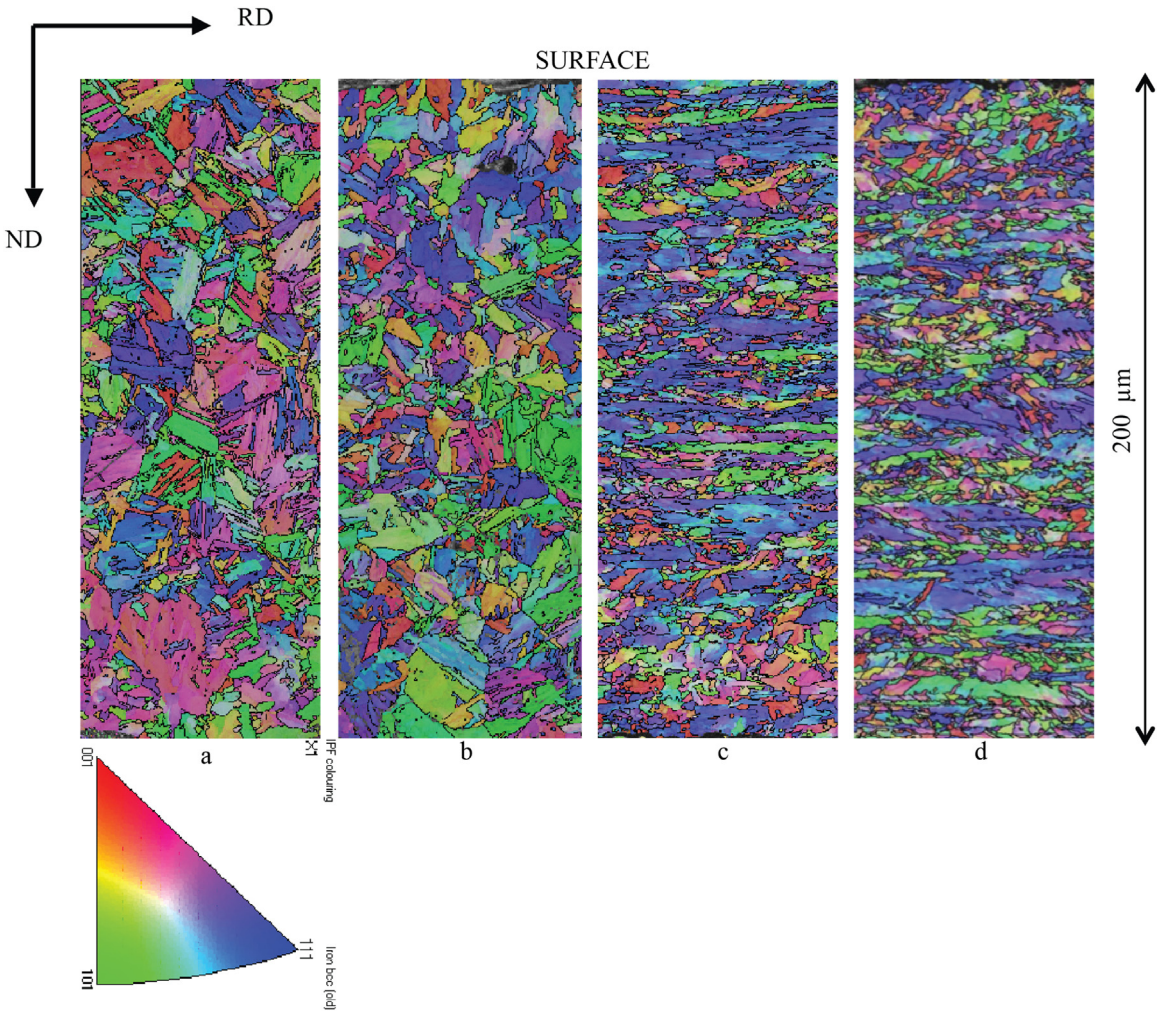

Fig. 3. Subsurface EBSD inverse pole figure maps for the RD direction for (a) RAQ, (b) RAQT (570 °C), (c) DQ and (d) DQT (570 °C) specimens. The sheet normal direction (ND) and the rolling direction (RD) in the cross-sections are shown.

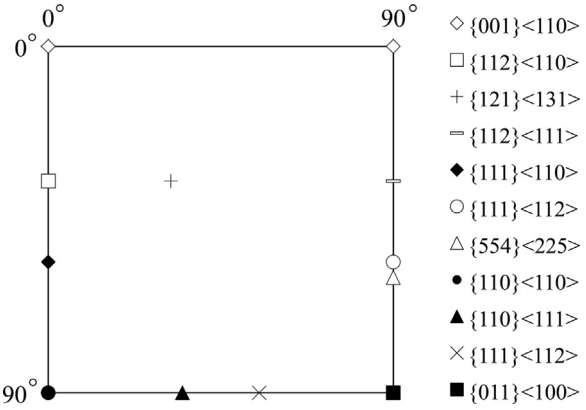

Fig. 4. The main texture components of the BCC structure in the $\varphi_2 = 45°$ ODF section.

condition has a higher intensity of misorientation angles in the range of 7.5–50°, while the RAQ condition shows a higher incidence of misorientation angles in the range of 50–58°. This is in line with the results of Zajac [19], which showed more random misorientation angle distribution in microstructures containing ferrite and granular bainite. Microstructure investigations showed that the RAQ condition is fully martensitic leading to a higher intensity of high-angle misorientation angles. For the tempered conditions, shown in Fig. 6b, slightly different misorientation angle distributions can be seen. While the DQ condition remains unchanged after tempering, the RAQ condition shows slight changes in the distribution profile with a lower incidence of low-angle boundaries below 7.5°. Caron and Krauss [17] have earlier shown that tempering rapidly decreases the incidence of low-angle boundaries in Fe-0.2 C martensite by eliminating the low-angle boundaries between laths with similar orientations.

The microstructure at the quarter-thickness position is representative of the bulk microstructure and it is mainly responsible for the overall strength and impact toughness of the experimental steels. EBSD-IPF maps for the RD direction in the direct-quenched samples (Fig. 7) show a fundamental difference between the RAQ and DQ conditions. Thermomechanical treatment followed by direct quenching resulted in an elongated grain structure (Fig. 7c-d) compared to the conventional re-austenitizing and quenching (Fig. 7a-b). Furthermore, the grain sizes defined by low-angle (> 2.5°) and high-angle (> 15°) grain boundaries are finer. This applies to both the mean equivalent circle diameter (ECD) grain sizes and the high-angle grain sizes at 90% in the cumulative grain size distributions, i.e. $d_{90\%}$ (Fig. 8). Any effect of tempering at 570 °C on grain structure is hardly visible in Fig. 7. However, the high-angle grain size at 90% in the cumulative grain size distribution (Fig. 8), i.e. $d_{90\%}$, implies that the grain size distribution might be somewhat coarser after tempering, especially in the case of the RAQ condition.

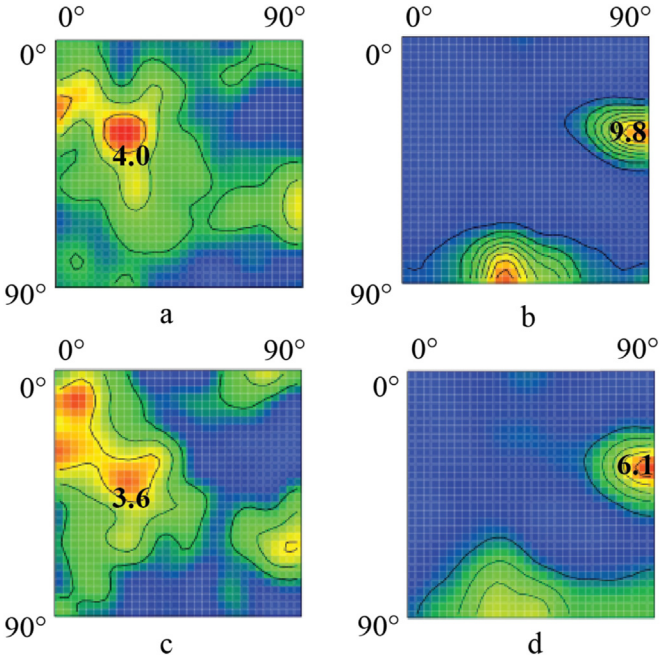

Fig. 5. φ_2 = 45° ODF sections presenting the subsurface textures from the depth of 0–0.45 mm below the surface for (a) RAQ, (b) DQ, (c) RAQT and (d) DQT steels. Tempering temperature 570 °C.

3.1.3. Dislocation density

Dislocation densities determined on the basis of X-ray diffraction line broadening using the Williamson-Hall method (WH) introduced in Eqs. 1–3 are presented in Fig. 9. As only one measurement was made for each condition, it is not possible to assign error bars to the data points. However, one measure of the uncertainty in the data is the goodness-of-fit obtained in the Rietveld refinement as discussed by Toby [24]. One method for analysing the data quality is to compare weighted profile R-factors (R_{wp}) to expected R factors R_{exp}, i.e the best possible value of R_{wp}. In a good fit R_{wp} should never be lower than R_{exp}, but not too much higher either. The present analyses showed R_{wp} values of 4–5% and R_{exp} values of 2–3% for all the data points, which indicates that the obtained fits were good. The trend in the estimated dislocation densities in Fig. 9 also appears quite smooth, which indicates that the relative errors involved are much smaller than the overall change.

The clear decrease in the dislocation density during tempering was found for all the experimental steels. The variation of dislocation density with tempering temperature shows that DQ martensite retains its dislocation density during tempering at 250 °C but that higher tempering temperatures lead to an ever increasing rate of decrease of the dislocation density especially above 400 °C. Despite having a slightly higher dislocation density in the as-quenched state, after tempering at 570 °C, the RAQ martensite has a slightly lower dislocation density than the DQ martensite. In other words, for the same tempering treatment, the RAQ condition suffers a higher decrease in dislocation density than the DQ condition with a deformed prior austenite grain structure. This observation is in line with the results from an earlier study [8] which showed that a larger austenite deformation below the recrystallization stop temperature before direct quenching raises the resistance of the bainitic–martensitic microstructure to loss of dislocation density during tempering. The prior austenite in the RAQ material will not be deformed and can be considered as representing austenite deformed entirely above the recrystallization temperature before direct quenching. Kennett [19,21] studied the effect of tempering RAQ martensite at 600 °C in a 0.20%C steel on the dislocation density determined using the same Williamson-Hall method as used here. Dislocation densities were in the range 8–10 × 10^{15} (m^{-2}) in the quenched condition, i.e. more than double those in Fig. 9, but 0.5–1 × 10^{15} (m^{-2}) after tempering at 600 °C, i.e. similar to those in Fig. 9. The doubly high carbon content of Kennett's steel compared to that studied here explains the roughly doubly higher initial dislocation density [22]. However, as with the present steel, Kennett's RAQ martensite does not seem to retain its dislocation density as well as DQ martensite. Kennett used micro-alloying elements in his study, but only 0.12%Mo which can have an effect on microstructural changes during tempering. Similarly, Takebayashi et al. [23] used the W-H method to study the effect of tempering temperature on the dislocation density of RAQ 0.3%C martensite. They found that the initial as-quenched dislocation density prior to tempering, 2 × 10^{16} (m^{-2}), was retained rather robustly until the tempering temperature reached 450 °C where it dropped to 1 × 10^{15} (m^{-2}) and even further to 0.5 × 10^{15} (m^{-2}) after tempering at 650 °C. These dislocation densities after tempering are similar to those seen here, despite the much higher untempered martensite dislocation density. Therefore, again it appears that the dislocation density of RAQ martensite is less resistant to tempering than that of DQ martensite. However, as Takebayashi studied composition including almost none of the elements commonly used to retard softening in tempering, definite conclusions cannot be made.

3.1.4. Mechanical properties

The effect of tempering temperature on yield and tensile strength are presented in Fig. 10. The results show that tempering at 200 °C and 400 °C causes a slight increase in yield strength. Compared to the as-quenched condition, tempering above 400 °C up to 600 °C causes a small decrease in yield strength but only with tempering at 650 °C is there a large decrease. For tempering at 570 °C, the RAQT condition has a lower yield strength than the DQT condition. This is understandable given the higher effective grain and lath size (Fig. 8) and lower dislocation density (Fig. 9) of the RAQT condition. However, in tensile strength, DQT and RAQT steels are similar i.e. DQT steels obtained clearly higher yield-to-tensile strength ratios. Even though yield strength differs between the DQT and RAQT conditions, the tensile

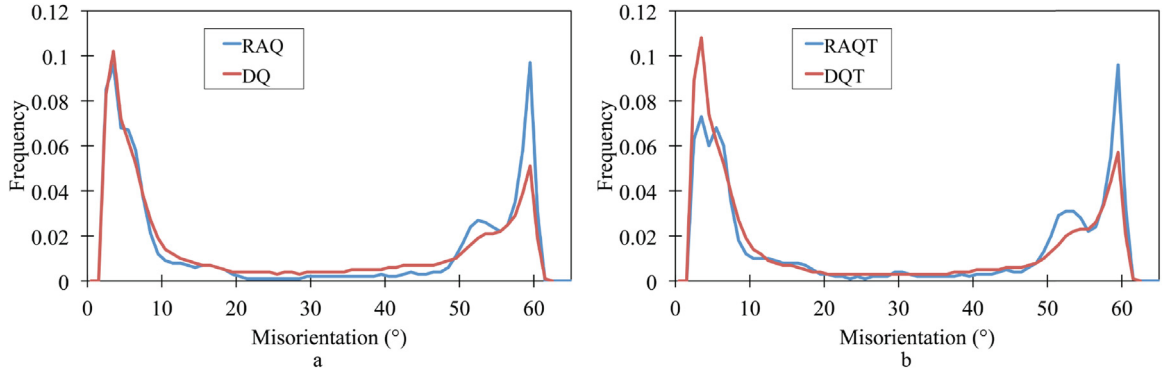

Fig. 6. Boundary misorientation distributions for the subsurface areas of (a) quenched and (b) quenched and tempered shown in Fig. 3.

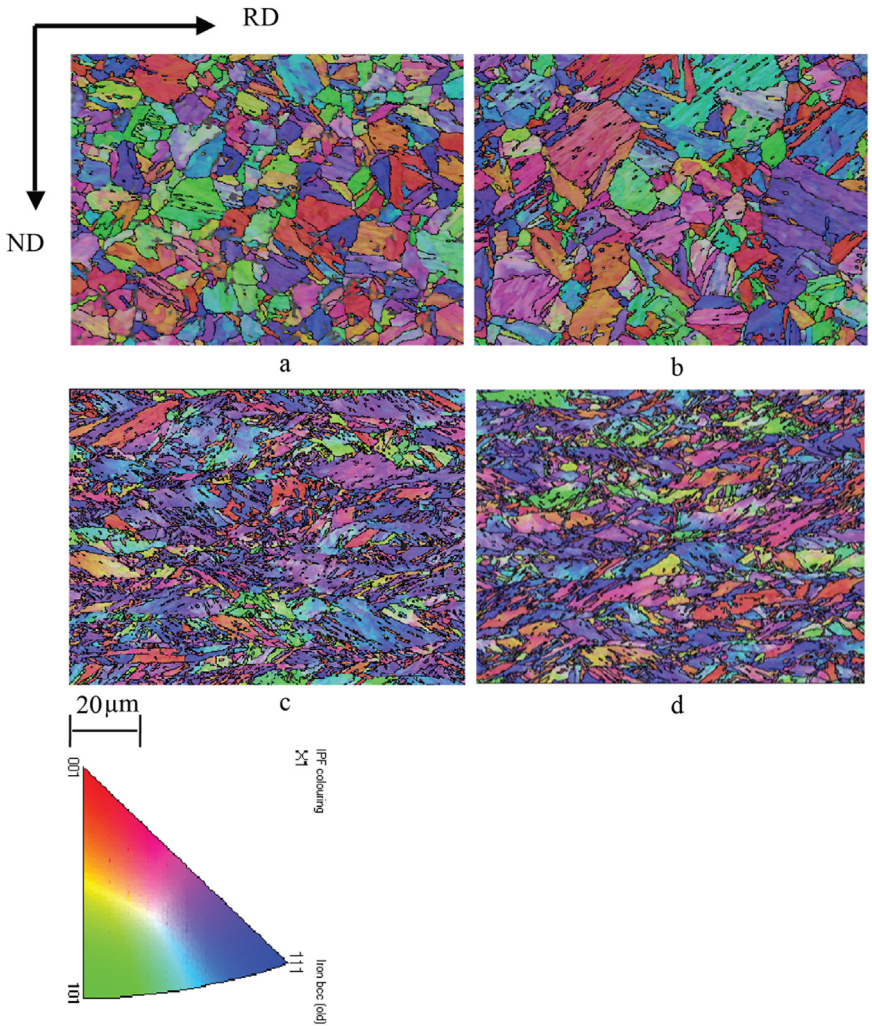

Fig. 7. Quarter thickness EBSD inverse pole figure maps for the RD direction for (a) RAQ, (b) RAQT, (c) DQ and (d) DQT steels. The sheet normal direction (ND) and the rolling direction (RD) in the cross-sections are shown.

strength, like hardness, seems to be independent of thermomechanical history, being mainly just a function of carbon content. This is in line with earlier results that show a clear correlation between carbon content and martensite hardness as well as a correlation between hardness and tensile strength [2].

Fig. 11 shows that uniform elongation is decreased with low temperature tempering, most likely due to the increase in yield strength (Fig. 10). However, it starts to increase rapidly when the tempering temperature is raised above 400 °C even though yield strength still remains at a similar level to the direct-quenched condition. The results also show that the condition of the austenite prior to quenching, i.e. RAQ or DQ, and the subsequent difference in texture and grain structure, has no effect on the uniform elongation or presumably work-hardening behavior.

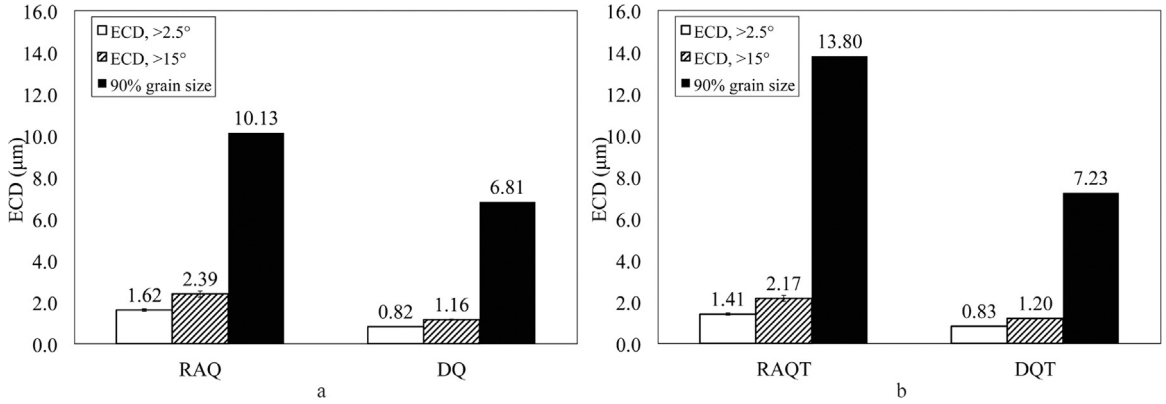

Fig. 8. Mean ECD grain and subgrain sizes and grain sizes at 90% in the cumulative grain size distribution for (a) RAQ and DQ steels and (b) RAQT and DQT steels. Tempering temperature 570 °C. Sub-grain sizes defined by misorientation angles > 2.5° and grain sizes by misorientation angles > 15°.

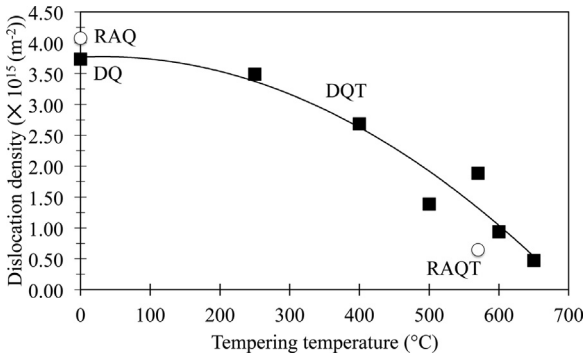

Fig. 9. The effect of tempering temperature and quenching condition on dislocation density. Open symbols show dislocation density of RAQ martensite and closed symbols DQ martensite. R_{WP} values of the used Rietveld refinement method was 4–5% for all measurements.

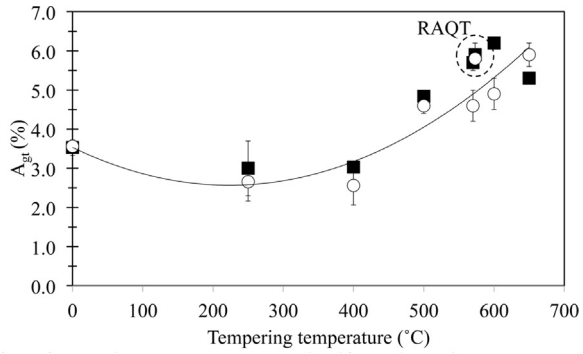

Fig. 11. The effect of tempering temperature on total uniform elongation. Open symbols transverse and closed symbols longitudinal specimens with respect to RD. Error bars show 95% confidence intervals for the means.

Fig. 12 shows that there is a linear correlation between uniform elongation and initial dislocation density. This is most likely due to an increased work hardening capacity with lower initial dislocation density.

The 28 J transition temperatures in different tempering conditions are presented Fig. 13. The results are clearly different to the reported behavior of higher carbon RAQ martensite, where embrittlement is seen after tempering in the range 300–500 °C and an improvement in toughness at higher temperatures [5]. However, for low-C DQ martensite, tempering causes embrittlement, i.e. an increase in impact toughness transition temperature, for all temperatures up to 600 °C. This is in line with earlier studies [8] showing that the good toughness of DQ martensitic-bainitic steels in the as-quenched state is not improved by tempering. Only after tempering at 650 °C is there an improvement in transition temperature with respect to the as-quenched state. In fact, the DQT material tempered at 650 °C, was so ductile that T28J could not be determined for the longitudinal test–the transition temperature was lower than the lowest testing temperature (−140 °C). The transition temperature of the RAQ condition was not tested in the study, but the RAQT condition showed possibly poorer toughness compared to the DQT condition for similar tempering conditions (570 °C). This was so despite the fact that the RAQT steel had a clearly lower yield strength, which, other things being equal, should lead to an improvement in the transition temperature [25].

Low toughness in the tempering range of 250–500 °C can be understood on the basis of the observed microstructural changes in the martensite. As the microstructures in Fig. 2 show, tempering in the 250–500 °C range results in the formation of long carbides in grain boundaries, which has been reported as being the cause of reduced toughness in the case of RAQ martensite [5]. Tempering at 570 °C and

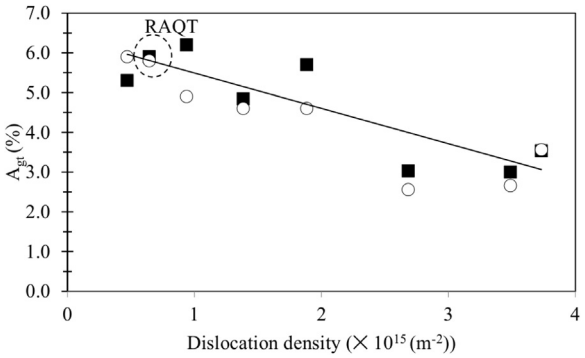

Fig. 12. Correlation between dislocation density and uniform elongation. Open symbols transverse and closed symbols longitudinal specimens with respect to RD.

above results in spheroidization of the carbides, which presumably reduces their embrittling potency.

For tempering with a peak temperature of 570 °C, the lower impact toughness, i.e. higher transition temperature, of the RAQT condition compared to the DQT condition seems to be due to the larger equiaxed grain structure of the RAQT microstructure. The fact that a fine elongated grain structure leads to improved toughness has been noted earlier, too [26,27].

It is clear from Fig. 13 that the transition temperature of transverse specimens is always higher than it is for longitudinal specimens. According to earlier findings, this anisotropy of impact toughness can be associated with texture effects [28,29].

In summary, the embrittlement of the present DQ martensite caused by tempering can be explained by the opposing effects of detrimental

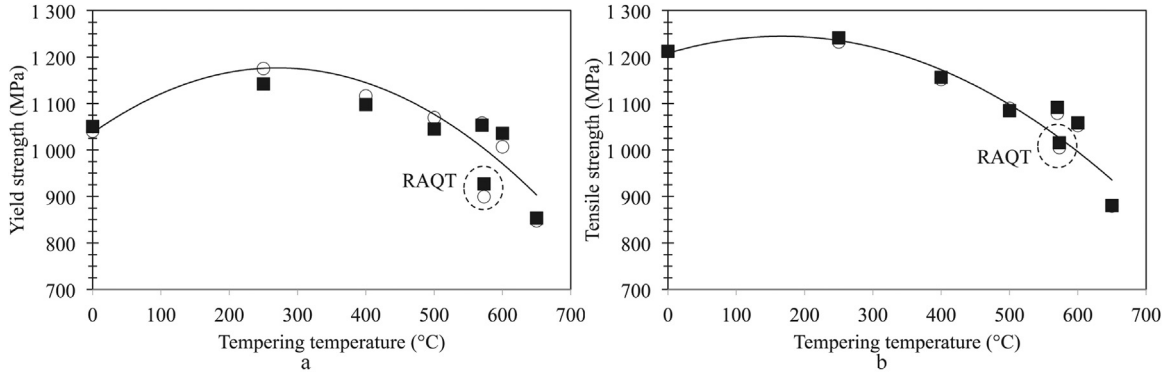

Fig. 10. Effect of tempering temperature on (a) yield and (b) tensile strength. Open symbols transverse and closed symbols longitudinal with respect to RD. RAQT results included for comparison. The 95% confidence intervals of the means are < 10 MPa for all points shown so error bars cannot be shown on the scale used.

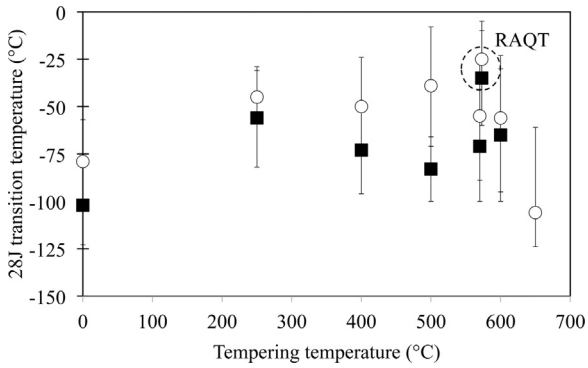

Fig. 13. The effect of tempering temperature on 28 J transition temperature. Open symbols transverse and closed symbols longitudinal specimens with respect to RD. Error bars show 95% confidence intervals for the means. The transition temperature of the longitudinal specimen tempered at 650 °C was below the lowest testing temperature (−140 °C) and could not be reliably determined.

elongated carbide precipitation and growth, on the one hand, and the beneficial effects brought about by lower yield stress, and perhaps spheroidization, on the other hand [25]. The failure of the DQT martensite to show an improvement in toughness up to a tempering temperature of 600 °C is probably due to the fact that the yield stress of the DQT condition is higher than that of the DQ condition up to almost 600 °C. Transition temperature is only improved after tempering at 650 °C at which the yield stress drops below that of the DQ condition.

3.1.5. Bendability

Results from the bendability tests are summarized in Fig. 14. Results show that the minimum bending radius is greatly affected by the tempering temperature. Bendability is isotropic for the as-quenched state and for the lowest and highest tempering temperatures, but in the tempering range 400–570 °C, bendability is better with the bend axis parallel to the RD. However, for the RAQT condition bendability is best with the bend axis transverse to the RD. Overall, tempering between 250 °C and 400 °C resulted in a reduction of bendability compared to the direct-quenched condition, while higher temperatures produced an improvement.

Earlier studies have also shown the strong effect of thermo-mechanical treatment on surface microstructure, texture and hardness of UHSS DQ steel [6,16,30]. In the present case the applied thermo-mechanical treatment, and therefore the texture and subsurface phase transformation characteristics, are not changed for DQ condition. Therefore, other factors must explain the observed changes in

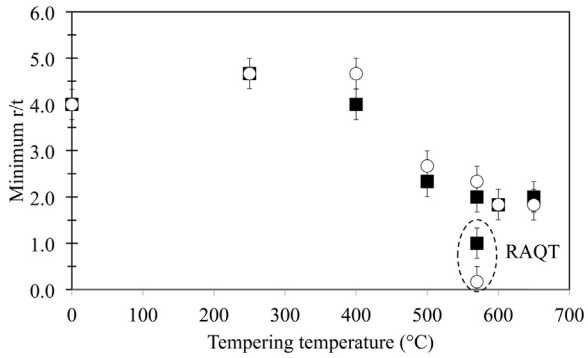

Fig. 14. The effect of tempering temperature on bendability, i.e minimum bending radius in persepective the sheet thickness, of DQ and RAQ steels. Open symbols bending axis in the transverse direction and closed symbols longitudinal direction relative to RD. Uncertainty of the minimum r/t is based on bending radius step size in the test.

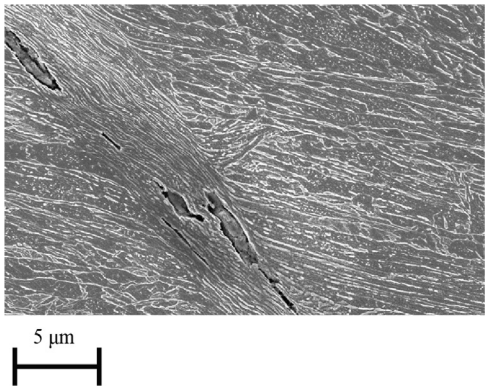

Fig. 15. FESEM image of shear band formation in DQ steel tempered at 570 °C. Bend axis transverse to rolling direction.

bendability. However, difference between DQT condition and RAQT can be explained by the different texture between these conditions (Fig. 5). As explained earlier, strong BCC shear components {112} < 111 > $_\alpha$, and {110} < 111 > $_\alpha$, are expected to form from the austenite close to rolled surfaces [18].

A strong shear texture component leads to planar anisotropy due to geometric softening and shear band formation when the bend axis is transverse to rolling direction (see Fig. 15) but not when axis is parallel to rolling direction. As mentioned above, similar behavior has also been reported earlier [6,16,30] explains the anisotropy in bending. Similarly, geometric softening explains the difference of DQT martensite to RAQT martensite as latter has different texture to DQT martensite, i.e. strong shear texture component is not present.

As tempering hardly affects the texture of the steels, the effect of tempering temperature on the bendability might be explainable in terms of either carbide distributions or initial dislocation density. Earlier work by Kaijalainen [16] showed the importance of subsurface microstructure and subsurface texture on the bendability of DQ steel. Long M-A islands and carbide regions along the RD were found to be especially detrimental to bendability, especially when the bend axis is transverse to RD. As the micrographs presented in Fig. 1 show, tempering at 250–400 °C leads to subsurface microstructures consisting of long carbide regions aligned along the rolling direction. As noted in earlier studies [20,21], long plate-like or needle-like M-A or carbide regions act as intensifiers of plastic strain in the matrix which can be detrimental especially to transverse bendability. As tempering temperature rises above 400 °C, the needle-like shape of the carbides is reduced through spheroidization, which may partly explain the improvement in bendability.

Earlier studies of a similar material to the present [6] showed, that for bainitic-martensitic microstructures, tempering led to improved bendability due to a decreased dislocation density and reduced hardness. As Fig. 16 show, there is a linear relationship between subsurface dislocation density and bendability in DQ condition. However, as Fig. 9 showed, dislocation density is not decreased linearly with rising tempering temperature: a clear drop in dislocation density is not observed until the tempering temperature is raised to 400 °C and above.

The linear relationship between uniform elongation and dislocation density (Fig. 12) leads to a linear relationship between bendability and uniform elongation, but only in the case of the DQ starting microstructure, as shown in Fig. 17. The RAQT steel clearly differs from the DQT steels obtaining much better bendability for a similar dislocation density and uniform elongation. Better bendability of RAQT steels are understood to be due to different surface texture and the absence of a strong shear texture component {112} < 111 > $_\alpha$ (Fig. 3 and Fig. 5) as presented earlier. Indeed, as the filled symbols in Fig. 16 show, when the bend axis is parallel to the RD, the RAQT material falls onto the same trend line as the DQ material. In other words, when the

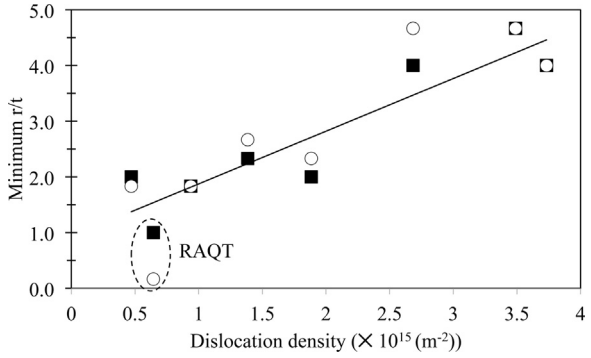

Fig. 16. Relationship between dislocation density and minimum bending radius. Open symbols bend axis transverse to RD, closed symbols bend axis parallel to RD.

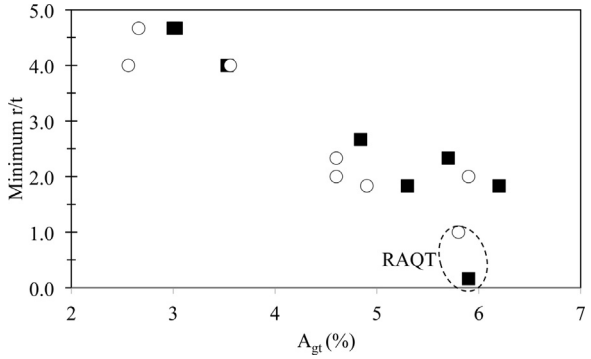

Fig. 17. Uniform elongation versus minimum bending radius. Open symbols bend axis transverse to RD (with longitudinal A_{gt}), closed symbols bend axis parallel to RD (with transverse A_{gt}).

detrimental effect of the {112} < 111 >$_\alpha$ texture component is absent, the DQT and RAQT materials behave in a similar way. Were it not for the presence of the detrimental {112} < 111 >$_\alpha$ texture component in the DQT material, the bendability around the transverse direction would be clearly better showing generally lower r/t ratios for all tempering conditions and dislocation densities.

Discussion above summarises the affecting factors on bendability of direct-quenched and tempered steels. Bendability of DQT steels is controlled by subsurface microstructure, dislocation density and texture. For direct-quenched steels, strong shear texture components form in the austenite close to the rolled surfaces, i.e., {111} < 211 >$_\gamma$ and {112} < 110 >$_\gamma$. After cooling and phase transformation these lead to the formation of the BCC shear components {112} < 111 >$_\alpha$, and {110} < 111 >$_\alpha$, respectively leading to shear band formation through geometrical softening in bending transverse to the RD. Respectively, subsurface microstructure is also mainly controlled by hot rolling and direct-quenching procedure, but as presented earlier, tempering temperature plays significant role on carbide structure formation and hardness changes during tempering in the surface of the strip. Third affecting factor, i.e. dislocation density, is strongly controlled by tempering temperature. High tempering temperatures lead to low dislocation density, uniform elongation and higher work hardening capacity. Difference between RAQT and DQT steels, in terms of bendability, origin from different texture in subsurface and therefore different behavior in transverse bending due to geometrical softening. This is inline with Dillamore's [30] findings that shear band formation depends on geometric softening and work hardening rate.

The results presented in current paper show that superior bendability and still high yield strength can be obtained when tempering temperature of DQ strip is selected so that uniform carbide structure is formed and dislocation density is decreased but yield strength is still retained at desired level. For current composition optimal balance was found when tempering temperature was 570–600 °C.

4. Summary and conclusion

The effect of tempering temperature on the microstructure and dislocation density of a specific low-carbon direct-quenched steel have been related to strength, toughness and bendability. Tempering was done using slow heating to a peak temperature followed by slow cooling to simulate the processing of large steel coils direct quenched on a hot strip mill. The tempering cycles are referred to in terms of their peak temperatures, which were 250, 400, 500, 570, 600 and 650 °C. To distinguish the effect of direct quenching as opposed to reheating and quenching, the properties of martensite formed from the same composition by conventional re-austenitizing, quenching and tempering have been examined for the peak temperature 570 °C. Based on the experimental results, the following conclusions can be drawn:

(1) Hot rolling in the no recrystallization temperature regime followed by direct quenching leads to a strong intensity of the shear texture component {112} < 111 >$_\alpha$ which is not present after re-austenitization and quenching.
(2) Dislocation density decreases as a function of tempering temperature, especially above 400 °C. This leads to higher uniform elongation and better bendability.
(3) The dislocation density of the DQ condition is less affected by tempering at 570 °C than the RAQ condition, despite the lower initial dislocation density of the DQ condition.
(4) Tempering temperature had remarkable effect on carbide structure both at the subsurface and quarter-thickness positions in the strip. To avoid the long carbide regions in the grain boundaries that are detrimental to both bendability and impact toughness transition temperature, tempering temperature had to be at least 570 °C or higher.
(5) The yield strength of the DQ strip was not compromised until tempering temperature exceeded 600 °C.
(6) Unlike medium-carbon RAQ martensite, the 28 J Charpy V transition temperature of low-carbon DQ martensite is increased by tempering even up to the tempering temperature of 600 °C. This is due to the detrimental effects of elongated grain boundary carbides, which are not alleviated by spheroidization and a substantial drop in yield strength until the tempering temperature exceeds 600 °C.
(7) The bendability of re-austenitized, quenched and tempered steel is better when the bend axis is transverse to rolling direction while for direct-quenched steel the opposite is true due to the detrimental effect of the shear texture component {112} < 111 >$_\alpha$, which is much stronger when quenching austenite deformed below its recrystallization temperature.
(8) Irrespective of the orientation of the bend axis, re-austenitized, quenched and 570 °C tempered steel has better bendability than direct-quenched and 570 °C tempered steel due to the lower dislocation density of the former and the strong shear texture component of the latter.
(9) Tempering increasingly improves bendability over the peak tempering temperature range 500–600 °C. The precipitation of long needle-like precipitates with tempering in the range 250–500 °C, both near the surface and deeper in the steel, partially counteracts the beneficial effects accruing from the reduction of the dislocation density.
(10) Raising the tempering temperature above 600 °C did not provide any further improvement in bendability, despite lower strength and improved toughness.

Acknowledgements

This work was made as a part Breakthrough Steels and Applications program of the Digital, Internet, Materials & Engineering Co-Creation, DIMECC Oy. The financial support of SSAB Europe Oy and The Finnish Funding Agency for Technology and Innovation (Tekes) is gratefully acknowledged (Grant no. 2137/31/2013).

Funding

This work was supported by the Finnish Funding Agency for Technology and Innovation (Tekes) and SSAB Europe Oy.

References

[1] G. Krauss, D.K. Matlock, Effects of strain hardening and fine structure on strength and toughness of tempered martensite in carbon steels, J. Phys. IV 5 (1995) 51–59.
[2] G. Krauss, Martensite in steel: strength and structure, Mater. Sci. Eng. A 273–275 (1999) 40–57.
[3] G. Krauss, Tempering of lath martensite in low and medium carbon steels: assessment and challenges, Steel Res. Int. 88 (10) (2017).
[4] S.C. Kennett, K.O. Findley, Strengthening and toughening mechanisms in martensitic steel, Adv. Mater. Res. 922 (2014) 350–355.
[5] R.M. Horn, R.O. Ritchie, Mechanisms of tempered martensite embrittlement in low alloy steels, Metall. Trans. A 9 (8) (1978) 1039–1053.
[6] A. Saastamoinen, A. Kaijalainen, D. Porter, P. Suikkanen, The effect of thermo-mechanical treatment and tempering on the subsurface microstructure and bendability of direct-quenched low-carbon strip steel, Mater. Charact. 134 (2017).
[7] K.W. Andrews, Empirical formulae for the calculation of some transformation temperatures, J. Iron Steel Inst. 20 (1965) 721–727.
[8] A. Saastamoinen, A. Kaijalainen, D. Porter, P. Suikkanen, J.-R. Yang, Y.-T. Tsai, The effect of finish rolling temperature and tempering on the microstructure, mechanical properties and dislocation density of direct-quenched steel, Mater. Charact. 139 (2018).
[9] G. Williamson, W. Hall, X-ray line broadening from filed aluminium and wolfram, Acta Metall. 1 (1) (1953) 22–31.
[10] G.K. Williamson, R.E. Smallman, III. dislocation densities in some annealed and cold-worked metals from measurements on the X-ray debye-scherrer spectrum, Philos. Mag. 1 (1) (1956) 34–46.
[11] W. Oldfield, Curve fitting impact test data: a statistical procedure, 1975.
[12] M.A. EricksonKirk, M.T. EricksonKirk, S. Rosinski, J. Spanner, A comparison of the tanh and exponential fitting methods for Charpy V-Notch energy data, J. Press. Vessel Technol. 131 (3) (2009) 31404–31413.
[13] K. Wallin, Mini- ja normaalikokoisten Charpy-V-koesauvojen tulosten välinen korrelaatio, VTT Res. Rep. 428 (1986) 31.
[14] K. Wallin, Fracture Toughness of Engineering Materials by Kim Wallin, Fracture Toughness of Engineering Materials., 2011.
[15] J. Heikkala, A. Väisänen, Usability testing of ultra high-strength steels, in: Proceedings of the 11th Biennial Conference on Engineering Systems Design and Analysis, 2012, pp. 1–13.
[16] A.J. Kaijalainen, P.P. Suikkanen, L.P. Karjalainen, D.A. Porter, Influence of subsurface microstructure on the bendability of ultrahigh-strength strip steel, Mater. Sci. Eng. A 654 (2016) 151–160.
[17] R.N. Caron, G. Krauss, The tempering of Fe-C lath martensite, Metall. Trans. 3 (9) (1972) 2381–2389.
[18] N.J. Wittridge, J.J. Jonas, The austenite-to-martensite transformation in Fe–30%Ni after deformation by simple shear, Acta Mater. 48 (10) (2000) 2737–2749.
[19] S. Zajac, V. Schwinn, K.H. Tacke, Characterisation and quantification of complex bainitic microstructures in high and ultra-high strength Linepipe steels, Mater. Sci. Forum 500–501 (2005) 387–394.
[20] S. Kennett, G. Krauss, K.O. Findley, Prior austenite grain size and tempering effects on the dislocation density of low-C Nb–Ti microalloyed lath martensite, Scr. Mater. 107 (2015) 123–126.
[21] S. Kennett, K. Findley, The strengthening and toughening mechanisms in ultra low carbon martensitic steel, in: THERMEC, 2013, pp. 350–355.
[22] S. Morito, J. Nishikawa, T. Maki, Dislocation density within lath martensite in Fe–C and Fe–Ni alloys, ISIJ Int. 43 (9) (2003) 1475–1477.
[23] S. Takebayashi, T. Kunieda, N. Yoshinaga, K. Ushioda, S. Ogata, Comparison of the dislocation density in martensitic steels evaluated by some X-ray diffraction methods, ISIJ Int. 50 (6) (2010) 875–882.
[24] B.H. Toby, R factors in rietveld analysis: how good is good enough? Powder Diffr. 21 (1) (2006) 67–70.
[25] J.F. Knott, Quantifying the quality of steel, Ironmak. Steelmak. 35 (2008) 264–282.
[26] A.J. Kaijalainen, P.P. Suikkanen, T.J. Limnell, L.P. Karjalainen, J.I. Kömi, D.A. Porter, Effect of austenite grain structure on the strength and toughness of direct-quenched martensite, J. Alloy. Compd. 577 (2013) S642–S648.
[27] A.J. Kaijalainen, P.P. Suikkanen, L.P. Karjalainen, J.I. Komi, A.J. DeArdo, Effect of austenite conditioning in the non-recrystallization regime on the microstructures and properties of ultra high strength bainitic/martensitic strip steel, in: Proceedings of the 2nd International Conference Super-High Strength Steels, 2010.
[28] X.L. Yang, Y.B. Xu, X.D. Tan, D. Wu, Influences of crystallography and delamination on anisotropy of Charpy impact toughness in API X100 pipeline steel, Mater. Sci. Eng. A 607 (2014) 53–62.
[29] X.L. Yang, Y.B. Xu, X.D. Tan, D. Wu, Relationships among crystallographic texture, fracture behavior and Charpy impact toughness in API X100 pipeline steel, Mater. Sci. Eng. A 641 (2015) 96–106.
[30] A. Kaijalainen, M. Liimatainen, V. Kesti, T. Liimatainen, A. David, Influence of composition and hot rolling on the subsurface microstructure and bendability of ultrahigh-strength strip, Metall. Mater. Trans. A (2016).